Double-Plane Image Reconstruction/Authentication Based on Double-Plane Phase Only Functions Located at Different Distances

Hsuan T. Chang[1], Mao S. Jhao[1]

htchang@yuntech.edu.tw
[1]Phonotics and Information Laboratory, Department of Electrical Engineering, National Yunlin University of Science and Technology, Yunlin Taiwan ROC

Keywords: Phase retrieval algorithm, Fresnel transform, double-plane image reconstruction, optical image authentication, phase only function

ABSTRACT

In this paper, we propose a method of using double-plane phase only functions (DPPOFs) and applying Fresnel diffraction transform to achieve double-plane image reconstruction/authentication. Based on the principle of optical Fresnel diffraction, we use the double phase retrieval algorithm to encode two target images at two different reconstruction planes into DPPOFs. The simulation results show that the two target images can be successfully reconstructed with good quality at the designated planes. The gradual image transition effects at the arbitrarily consecutive reconstruction planes within the two designated planes can also be observed.

1 Introduction

Recently, with the rapid development of Internet technology, the distributions of texts, images and audio-visuals are easier and more convenient. However, it also makes people realize that some signification information becomes easier to be stolen, modified, or even can be made into counterfeit products by unscrupulous people. Therefore, important information must be avoided being stolen or even illegally used by criminals. This is already a very important issue in network technology.

In the past few decades, two important issues in the field of computer generated holography (CGH): numerical generation and encryption, have been continuously discussed and studied. In 1995, Refregier and Javidi first proposed to use two random phases to encrypt the image [1]. Since then, a series of optical image encryption and authentication methods have developed based on this concept [2, 3].

Based on the previous multiple-phase retrieval algorithm (MPRA) [4], we propose a double-plane image reconstruction and authentication method. First, we modify the Fourier transform used in MPRA as a Fresnel transform (FrT). Next, we consider the optical architecture shown in Fig. 1, in which two images are encrypted into two POFs, all at two planes with different distances along the optical axis. The first POF is Fresnel transformed at the second plane and then is multiplied by the second POF to obtain the composite light field. Then we apply the FrT to obtain the light field at the designated image plane. The amplitude is modified according to the target image constrain, and its inverse FrT is used to obtain double-plane POFs (DPPOFs) at the two distances. We use the DPPOFs obtained from the first target image to perform Fresnel operation but change the distance coefficient. Based on the second target image at the second position we set, we modify the amplitude according to the second target image and use inverse FrT to obtain DPPOFs at the two planes. The above process is an iterative operation and will not stop until the reconstructed images converge to the desired target images. The optical architecture using FrT can obtain the better flexibility on parameter modification than that using Fourier transform. The final POFs can also serve as the encryption data of the two target images and are also more secure than the system using just one POF for one target image reconstruction.

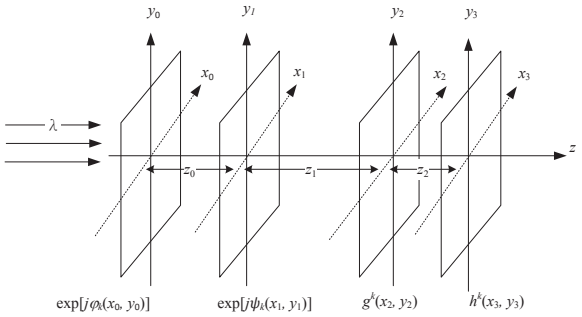

Fig. 1 Optical architecture for two POFs and two target images at different planes

2 Proposed Method

Equation (1) shows the definition of FrT between two planes (x, y) and (x_0, y_0):

$$A(x,y) = \mathrm{FrT}\{a(x_0,y_0)\} = \frac{\exp(\frac{j2\pi z}{\lambda})}{j\lambda z} \iint g(x_0,y_0) \times \exp\{\frac{j\pi}{\lambda z}[(x-x_0)^2 + (y-y_0)^2]\}\, dx_0 dy_0, \quad (1)$$

where (x_0, y_0) is the coordinate of the POF plane, (x, y) is the coordinate of the diffraction plane, λ is the

wavelength of light incident into (x_0, y_0) plane, and z is the distance between the POF and diffraction plane with coordinate (x, y). Figure 2 shows the systematic diagram of the proposed iterative algorithm especial for the proposed double-plane POFs retrieval. First, we generate two POFs $\varphi_k(x_0, y_0)$ and $\psi_k(x_1, y_1)$ whose phase signals are randomly distributed within 0 and 2π and initially k=0. Based on Fig. 1 and Eq. (1), the complex light field distribution $g^k(x_2, y_2)$ can be determined using Eq. (2)

$$g^k(x_2, y_2) = \mathrm{FrT}\{\mathrm{FrT}\{\exp[j\varphi_k(x_0, y_0)]; \lambda; z_0\} \times \exp[j\psi_k(x_1, y_1)]; \lambda; z_1\}, \quad (2)$$

where z_0 is the distance between the two POFs, z_1 is the distance between the POF $\psi_k(x_1, y_1)$ and the first target image plane (x_2, y_2). Next, the amplitude of the complex light filed $g^k(x_2, y_2)$ is replaced by the target image while the phase is preserved. To determine the POF $\psi_{k+1}(x_1, y_1)$ at next stage, the light distribution $g^k(x_2, y_2)$ is inversed Fresnel transformed and is divided by the FrT of the POF $\varphi_k(x_0, y_0)$ as shown in Eq. (3):

$$\psi_{k+1}(x_1, y_1) = \arg\{\frac{\mathrm{IFrT}\{g^k(x_2, y_2)\}}{\mathrm{FrT}\{\exp[j\varphi_k(x_0, y_0)]; \lambda; z_0\}}\} \quad (3)$$

The updated POF $\psi_{k+1}(x, y)$ is multiplied by the Fresnel transformed $\varphi_k(x_0, y_0)$ and again transformed to the first target image plane (x_2, y_2). Then the updated light field can be expressed by Eq. (4):

$$g^{k+1}(x_2, y_2) = \mathrm{FrT}\{\mathrm{FrT}\{\exp[j\varphi_k(x_0, y_0)]; \lambda; z_0\} \times \exp[j\psi_{k+1}(x_1, y_1)]; \lambda; z_1\} \quad (4)$$

The amplitude is then replaced by the target image due to the image plane constraint. This modified light field is then inversely Fresnel transformed and divided by the POF $\psi_{k+1}(x_1, y_1)$. Equation (5) shows the process of determining the POF $\varphi_{k+1}(x_0, y_0)$,

$$\varphi_{k+1}(x_0, y_0) = \arg\{\mathrm{IFrT}\{\frac{\mathrm{IFrT}\{g^{k+1}(x_2, y_2)\}}{\exp[j\psi_{k+1}(x_1, y_1)]}; \lambda; z_0\}\} \quad (5)$$

The second target image $h^k(x_3, y_3)$ can be determined based on the updated POFs $\varphi_{k+1}(x_0, y_0)$ and $\psi_{k+1}(x_1, y_1)$. Equation (6) shows the FrT processes applied to the two POFs:

$$h^k(x_3, y_3) = \mathrm{FrT}\{\mathrm{FrT}\{\exp[j\varphi_{k+1}(x_0, y_0)]; \lambda; z_0\} \times \exp[j\psi_{k+1}(x_1, y_1)]; \lambda; z_1 + z_2\}, \quad (6)$$

where $z_1 + z_2$ is the distance between the POF $\psi_{k+1}(x_1, y_1)$ and the second targe image plane, $h^k(x_3, y_3)$ is the complex light field distributed at the second target image plane. The image plane constraint is applied to the amplitude of the light field $h^k(x_3, y_3)$, which is then used to determine the (k+2)th POF $\psi_{k+2}(x_1, y_1)$ based on Eq. (7):

$$\psi_{k+2}(x_1, y_1) = \arg\left\{\frac{\mathrm{IFrT}\{h^k(x_3, y_3)\}}{\mathrm{FrT}\{\exp[j\varphi_{k+1}(x_0, y_0)]; \lambda; z_0\}}\right\} \quad (7)$$

With this new POF $\psi_{k+2}(x_1, y_1)$ and the other POF $\varphi_{k+1}(x_0, y_0)$, we again determine the (k+1)th light field distribution $h^{k+1}(x_3, y_3)$ at the second target image plane by using Eq. (8):

$$h^{k+1}(x_3, y_3) = \mathrm{FrT}\{\mathrm{FrT}\{\exp[j\varphi_{k+1}(x_0, y_0)]; \lambda; z_0\} \times \exp[j\psi_{k+2}(x_1, y_1)]; \lambda; z_1 + z_2\} \quad (8)$$

Again, the image plane constraint is applied to the amplitude of the light field $h^{k+1}(x_3, y_3)$, which is then used to determine the (k+2)th POF $\varphi_{k+2}(x_0, y_0)$ based on Eq. (9):

$$\varphi_{k+2}(x_0, y_0) = \arg\{\mathrm{IFrT}\{\frac{\mathrm{IFrT}\{h^k(x_3, y_3)\}}{\exp[j\psi_{k+2}(x_1, y_1)]}; \lambda; z_1 z_2\}\} \quad (9)$$

During the iteration process, the errors of the two reconstructed images at the two planes are examined. For example, the mean squared error (MSE) ε between the reconstructed and target images can be determined by using Eq. (10):

$$\varepsilon = \frac{1}{M \times N} \sum_{x=1}^{M} \sum_{y=1}^{N} [g(x_0, y_0) - g^k(x_0, y_0)]^2 \quad (10)$$

As shown in Eq. (11), when the MSE value ε_{k+1} is less than a threshold value γ, then the iteration process converges. Otherwise, the amplitude of the iterated light field distribution is replaced by the target image.

$$g^{k+1}(x_2, y_2) = \begin{cases} \bar{g}^{k+1}(x_2, y_2), & \text{if } \varepsilon_{k+1} \le \gamma \\ g(x_2, y_2), & \text{if } \varepsilon_{k+1} > \gamma \end{cases} \quad (11)$$

When both the two reconstructed images converge, the final two POFs at two planes can be obtained and are denoted as $\hat{\varphi}(x_0, y_0)$ and $\hat{\Psi}(x_1, y_1)$. The final two reconstructed images $\hat{g}(x_2, y_2)$ and $\hat{h}(x_3, y_3)$ are determined by using Eqs.(12) and (13), respectively.

$$\hat{g}(x_2, y_2) = \mathrm{FrT}\{\mathrm{FrT}\{\exp[j\hat{\varphi}(x_0, y_0)]; \lambda; z_0\} \times \exp[j\hat{\Psi}(x_1, y_1)]; \lambda; z_1\} \quad (12)$$

$$\hat{h}(x_3, y_3) = \mathrm{FrT}\{\mathrm{FrT}\{\exp[j\hat{\varphi}(x_0, y_0)]; \lambda; z_0\} \times \exp[j\hat{\Psi}(x_1, y_1)]; \lambda; z_1 + z_2\} \quad (13)$$

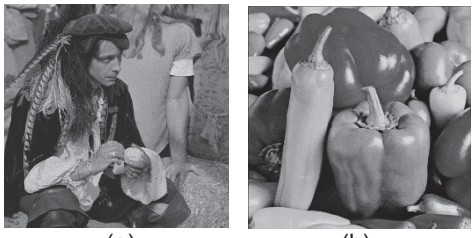

(a) (b)

Fig. 3. Two target images: (a) Indian; (b) Peppers

3 Simulation Results

The PC specifications are Intel(R) Core(TM) i5-4570 CPU@3.20 GHz, 8G DDR3 RAM, and Windows 10 operation system. Matlab R2019b serves as the coding platform in our simulation. Figure 3 shows two target images of size 512*512 used in our computer simulation. The parameters used in Fig. 1 are z_0=2 m, z_1=1 m, z_2=0.5 cm, wavelength λ =532 nm and the pitch size of SLM is 6.8 nm. In addition to the two target image planes, we also reconstruct the images every 0.1cm between the two image planes. Figures 4(a) to 4(e) show the reconstructed images at the planes of six distances. We can observe that the four intermediate images are aggressively modified from the first target image to the second one. The correlation coefficient (CC) value $\boldsymbol{\rho}$ defined in Eq. (14) is used to represent the image quality.

$$\rho = \frac{E\{[g-E[g]][|\hat{g}|-E[|\hat{g}|]]\}}{\sqrt{\left\{E\left\{[g-E[g]]^2\right\}E\left\{[|\hat{g}|-E[|\hat{g}|]]^2\right\}\right\}}}, \quad (14)$$

where $E[\cdot]$ denotes the expectation operator, g and $\hat{g}$ denote the original and reconstructed target images, respectively. When the value ρ is closer to 1.0, the reconstructed image is more similar to the target image. Table 1 shows the CC values of the reconstructed images at different distances between 1.3 m and 1.305 m. The CC values at the two target image planes are greater than 0.88, while the values at the other distances are much lower.

In Figs. 5(a) and 5(b), we also investigate effects on the CC values of the reconstructed images under the different distances z_0 between the two POFs. As shown in both figures, the longer distance z_0 leads to the lower CC values of the intermediate images reconstructed at the other distances. If we want to reconstruct the intermediate images with higher CC values to the two target images, then a shorter distance z_0, can be preferred. The transition effect from the first target image to the second one might be observed.

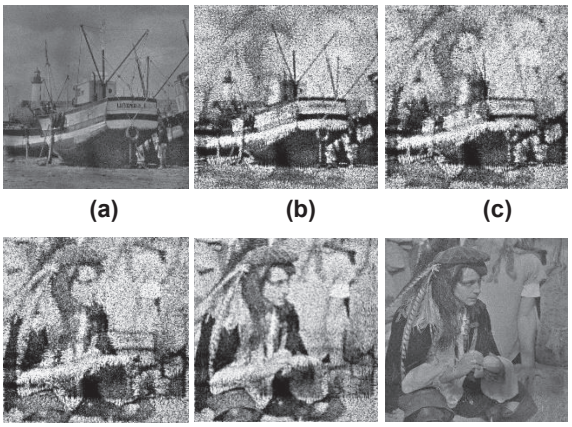

Fig. 4. Aggressively reconstructed images at various planes: (a) first target image plane; (b) 0.1 cm from (a); (c) 0.2 cm from (a); (d) 0.3 cm from (a); (e) 0.4 cm from (a); (f) second target image plane

Table 1. CC values (ρ) of the images reconstructed at the planes with different distances to POF ψ

Distance (m)	CC value
1.300	0.887
1.301	0.246
1.302	0.360
1.303	0.494
1.304	0.653
1.305	0.883

4 Conclusions

We develop a novel DPPOFs for double image reconstruction system based on FrT theory. The DPPOFs can be retrieved using the proposed iteration algorithm. The computer simulation results show that the two target images at the two designated planes can be successfully reconstructed with good quality. The proposed method can also be considered as an authentication method since two target images are encoded as DPPOFs. The image transition effects between two image planes based on different distances between two POFs are also investigated. In our future work, we will extend the capability of current method so that various numbers of POFs and target images can be selected.

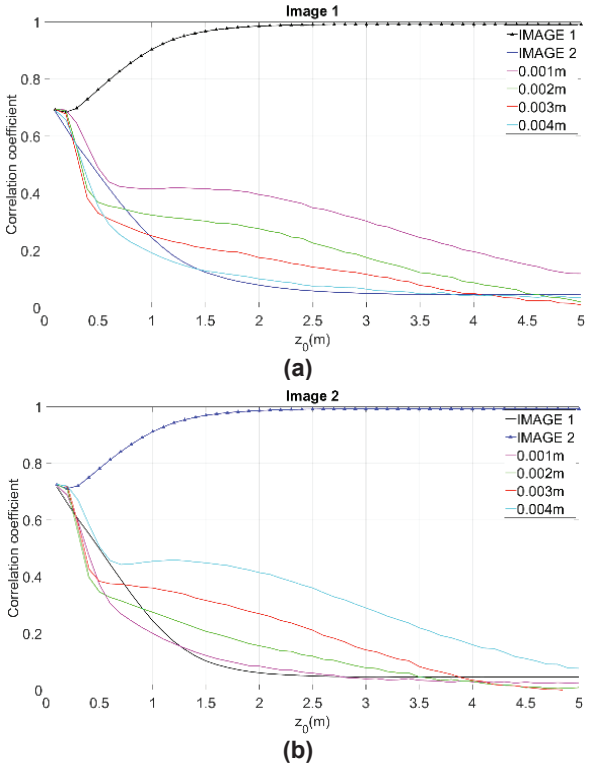

Fig. 5. The effects of using different distance z_0 between two POFs on the CC values of the two reconstructed target images: CC values of the images reconstructed at the planes under the six distances based on the (a) first and (b) second target images.

Acknowledgements

This research is partially supported by the National Science and Technology Council under the contract number: MOST 111-2221-E-224-023-MY2.

References

[1]. P. Refregier and B. Javidi, "Optical image encryption based on input plane and Fourier plane random encoding," Optics Letters, vol. 20, pp. 767-769, 1995.

[2]. S. Liu, C. Guo, and J. T. Sheridan, "A review of optical image encryption techniques," Optics & Laser Technology, vol. 57, pp. 327-342, Apr. 2014.

[3]. W. Chen, B. Javidi, and X. Chen, "Advances in optical security systems," Advances in Optics and Photonics, vol. 6, no. 2, pp. 120-155, 2014.
[4]. H.T. Chang, W.C. Lu, and C.J. Kuo, "Multiple-phase retrieval for optical security systems using random phase encoding," Applied Optics, vol. 41, no. 23, pp. 4825~4834, Aug. 2002.

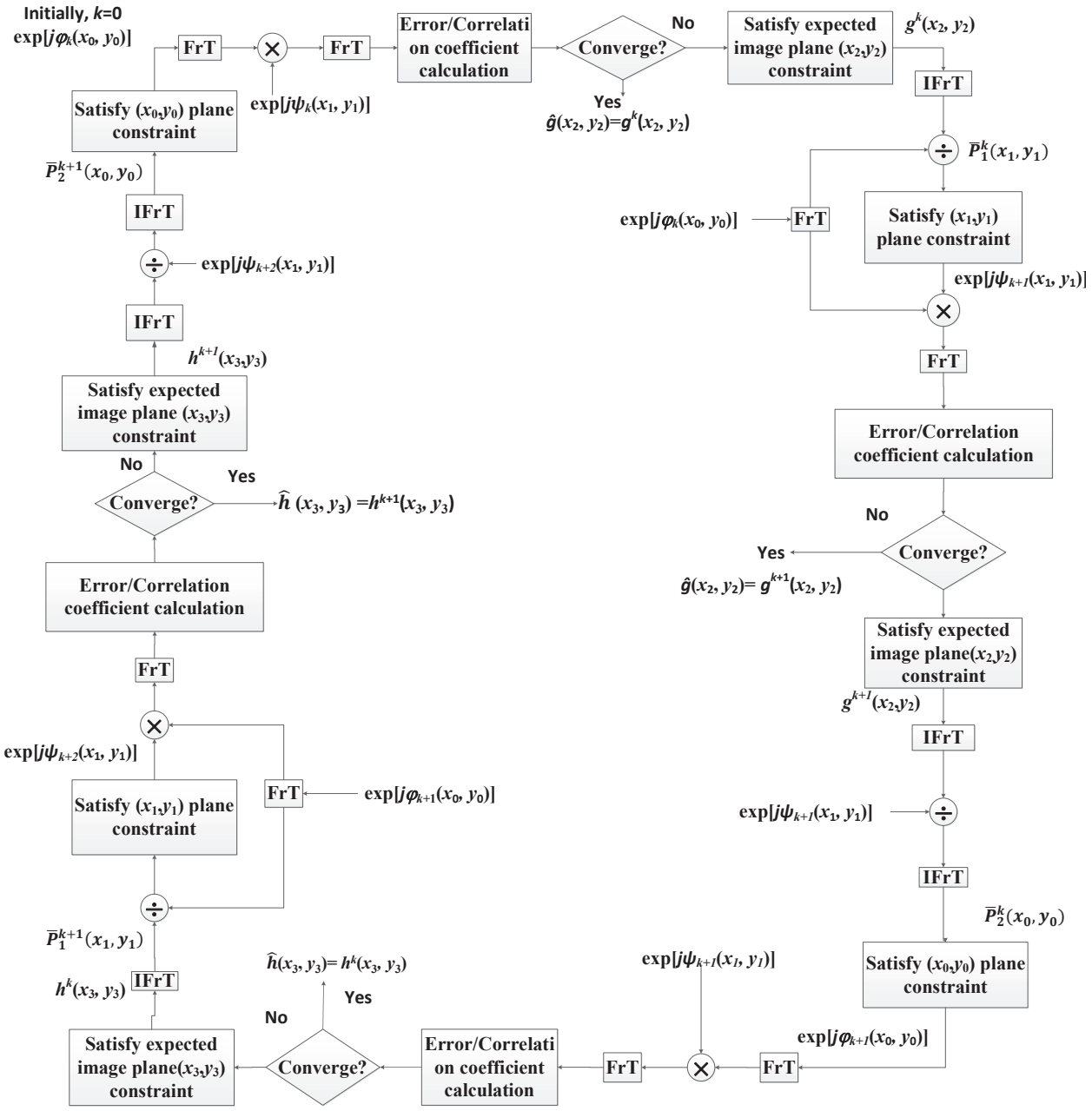

Fig. 2 Systematic diagram of the proposed iterative algorithm for DPPOF retrieval of two target images at different distances